Supporting information

Carbon-supported Zn-HPW ligand catalysts for acetylene hydration

Zhen Chen [a], Dingjie Luo [a], Qinqin Wang [a, *], Long Zhou [a], Yufan Ma [a], Fangjie Lu [a, *], Bin Dai [a, *]

a School of Chemistry and Chemical Engineering, Shihezi University/State Key Laboratory lncubation Base for Green Processing of Chemical Engineering, Shihezi 832000, China

Corresponding authors E-mail addresses: wqq_shzu@sina.com (Q. Wang); lfj_echo@shzu.edu.cn (F. Lu); db_tea@shzu.edu.cn (B. Dai).

Table of content

1. Computational methods

To obtain the relative energies along the reaction pathways, zero-point energy corrections were applied to all optimized configurations at the same level of optimization. The calculations also considered the Basis Set Superposition Error. During the geometry optimizations, no symmetry constraints were imposed, allowing for unrestricted exploration of the conformational space.

All geometries for the minima and transition states were calculated in the gas phase. Additionally, the study involved calculating the adsorption energy (E_{ads}) and co-adsorption energy ($E_{co\text{-}ads}$). These energies were defined as follows:

(1) $E_{ads} = E_{ads\text{-}state} - (E_{C2H2/H2O} + E_{catalyst})$

(2) $E_{co\text{-}ads} = E_{co\text{-}ads\text{-}state} - (E_{C2H2} + E_{H2O} + E_{catalyst})$

The $E_{C2H2/H2O+catalyst}$ represents the total energy of the system when either H_2O or C_2H_2 is adsorbed on the catalyst. On the other hand, the $E_{C2H2+H2O+catalyst}$ is the total system adsorption energy when both reactants are adsorbed on the catalyst. Additionally, E_{C2H2}, E_{H2O}, and $E_{catalyst}$ refer to the energy of the isolated C_2H_2 molecule, H_2O molecule, and the catalyst, respectively.

To validate that the correct products were associated with the corresponding reactants, Intrinsic Reaction Coordinate (IRC) calculations were performed [1-4]. IRC calculations are used to confirm that the reaction pathway connects the correct initial and final states.

2. Characterization analysis

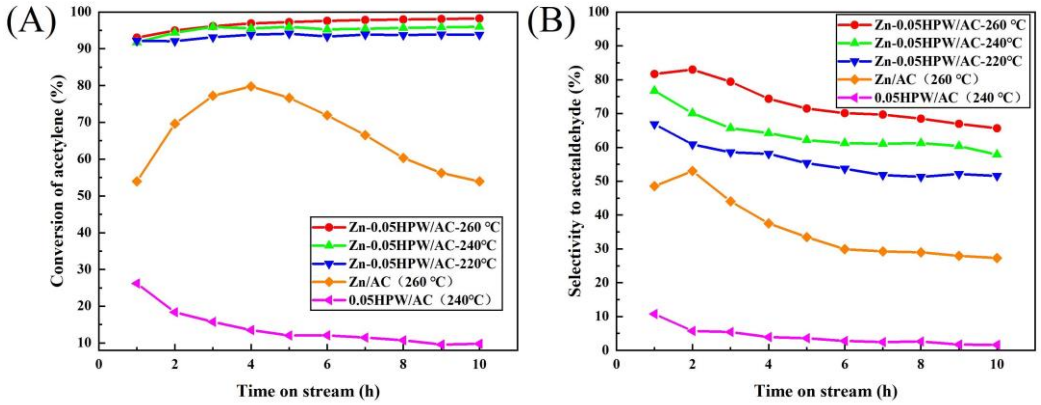

Fig. S1. Optimization of reaction temperature: (A) acetylene conversion; (B) acetaldehyde selectivity.

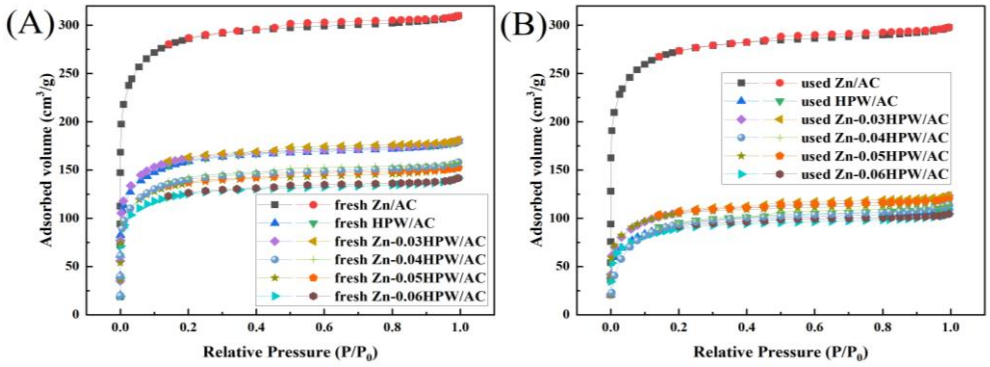

Fig. S2. N_2 adsorption-desorption isotherms of fresh (a) and used (b) catalysts

Table S1 Physical structure parameters of the catalysts

Catalysts	S_{BET} (m^2/g)		V (cm^3/g)		D (nm)	
	fresh	used	fresh	used	fresh	used
Zn/AC	920.6	879.8	0.48	0.46	2.8	2.9
HPW/AC	519.3	453.9	0.28	0.17	2.9	2.9
Zn-0.03HPW/AC	524.6	349.5	0.28	0.19	3.0	3.0
Zn-0.04HPW/AC	457.5	411.3	0.30	0.21	2.9	3.0
Zn-0.05HPW/AC	441.3	342.1	0.24	0.18	3.0	3.1
Zn-0.06HPW/AC	406.1	295.9	0.22	0.16	3.1	3.0

Fig. S2 and **Table S1** show the N_2 adsorption-desorption isotherms and physical structure parameters of all catalysts, respectively. All catalysts exhibit type I adsorption isotherms for mesoporous materials. The presence of hysteresis loops

between P/P_0=0.4 and 1.0 for both fresh and used catalysts implies the mesoporous structure of the carriers. After 10 h of reaction, both fresh and reacted catalysts maintained the mesoporous structure of the carriers. The pore structure parameters of fresh and used catalysts are shown in **Table S1**, and it can be found that the pore volume and specific surface area of the carriers decreased significantly after the addition of ligands, which may be due to the occupation of the carrier pore channels by the complexes formed by Zn and HPW.

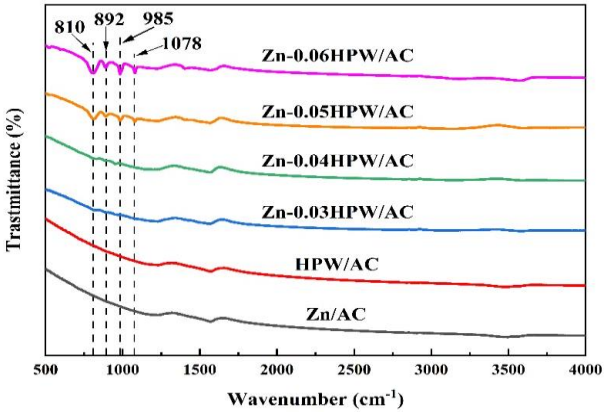

Fig. S3. FT-IR spectra of the fresh catalysts.

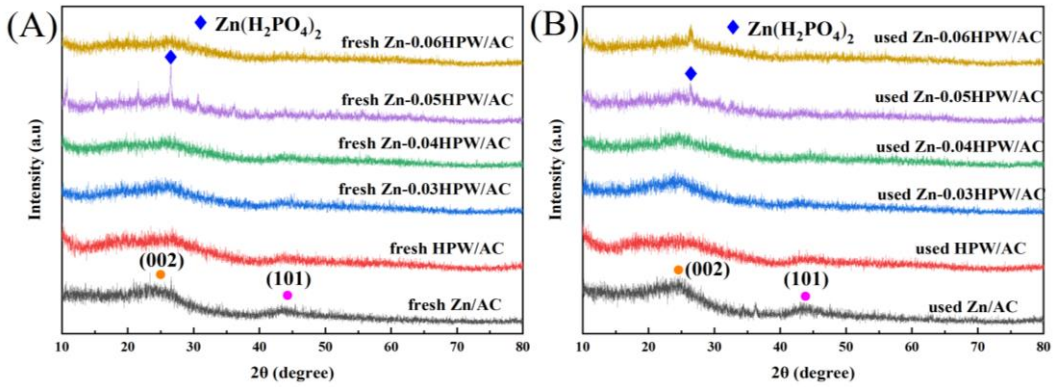

Fig. S4. XRD spectra of fresh (a) and used (b) catalysts

Fig. S4 shows the wide angle XRD spectra of the different catalysts. A comparison shows that all catalysts have very broad diffraction peaks around 24.8 ° and 43.7 °, which are attributed to the (002) and (101) crystal planes of the activated carbon [5], indicating that the introduction of HPW ligands did not disrupt the mesoporous structure of the carriers, which is consistent with the BET characterization. Furthermore, with increasing ligand content, a diffraction peak of $Zn(H_2PO_4)_2$ appeared at 2θ = 26.5 °, which could be attributed to the formation of

$Zn(H_2PO_4)_2$ by combining part of the HPW with Zn when an excess of ligand was introduced.

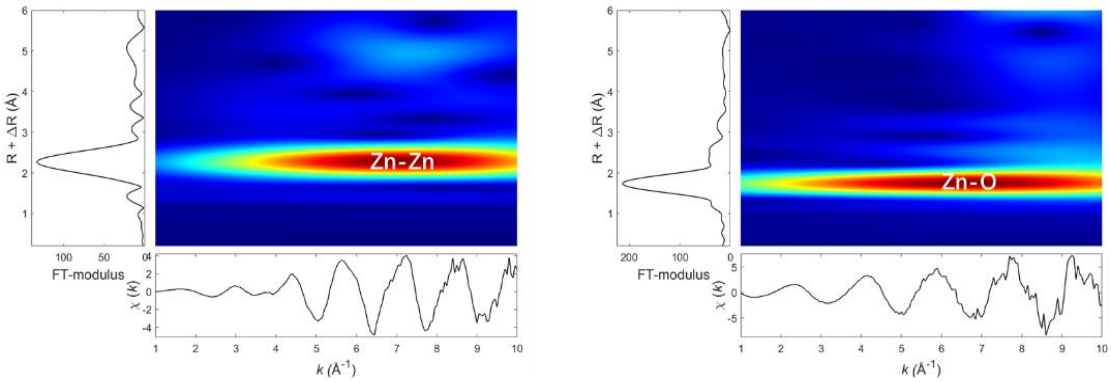

Fig. S5. Wavelet transform spectrum of the sample

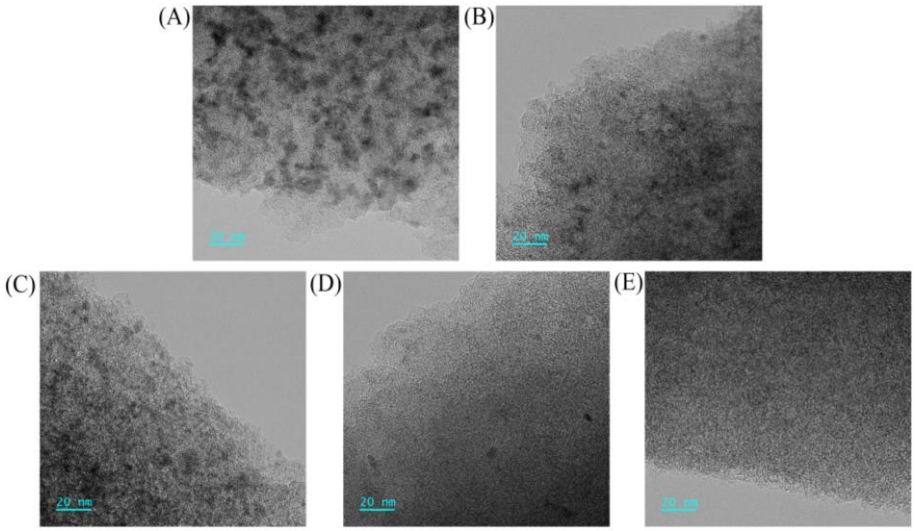

Fig. S6. TEM images of the used catalysts: Zn/AC (A), Zn-0.03HPW/AC (B), Zn-0.04HPWAC (C), Zn-0.05HPW/AC (D), Zn-0.06HPW/AC (E).

Table S2 Loading of Zn in the catalysts.

Catalysts	Content Zn (wt%)	Loss Zn (%)
Zn/AC	6.54%	11.31%
used Zn/AC	5.80%	
Zn-0.05HPW/AC	6.24%	5.29%
used Zn-0.05HPW/AC	5.91%	

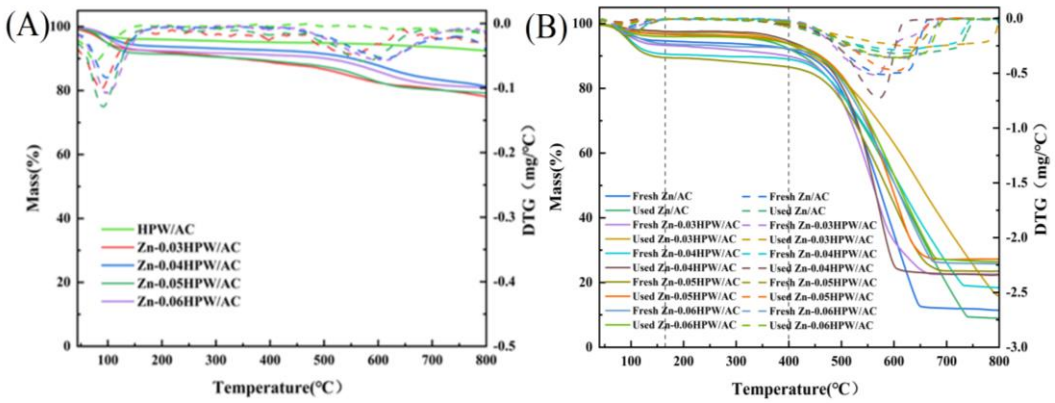

Fig. S7. Thermal stability curve (A) and thermogravimetric curve (B) of fresh catalyst.

Thermal stability tests were conducted under an N_2 atmosphere to investigate the stability of the fresh ligand catalyst. The results are shown in **Fig. S7(A)**. Samples experienced significant mass loss between room temperature and 150 ℃. The observed mass loss can be attributed to the evaporation of water absorbed by the catalyst samples upon exposure to air [6]. The fresh HPW/AC catalysts showed minimal decomposition of the HPW ligands, as evident from the TG curves. Between 400 ℃ and 800 ℃, the mass loss that occurred is probably due to the decomposition of the complexes formed by the HPW ligand with the Zn component. Based on these analysis results, the Zn-xHPW/AC (x=0.03, 0.04, 0.05, 0.06) catalysts exhibited good thermal stability, and their Zn complexes did not decompose at a reaction temperature of 260 ℃.

3. Comparison of configurations and adsorption energies at different H-atom positions

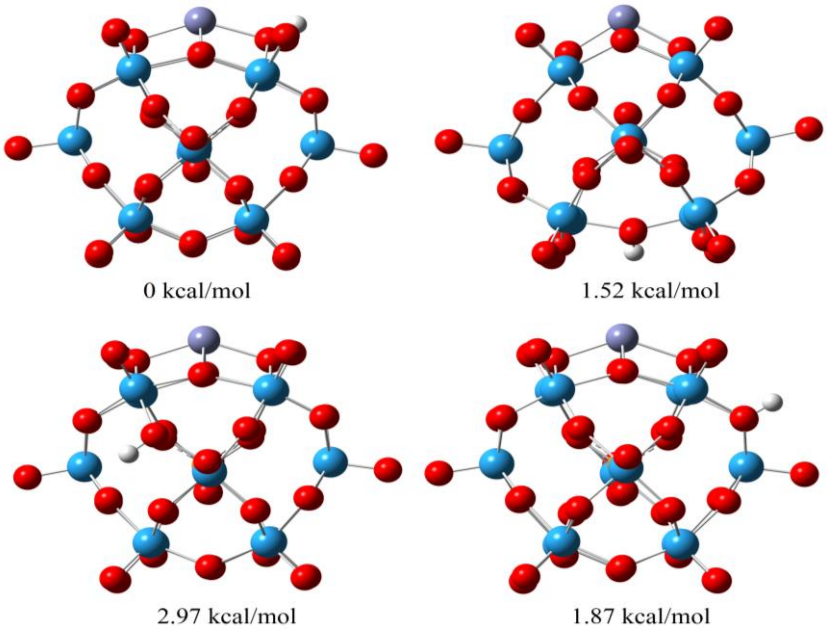

Fig. S8. Comparison of energies for different H-atom position configurations in catalysts.

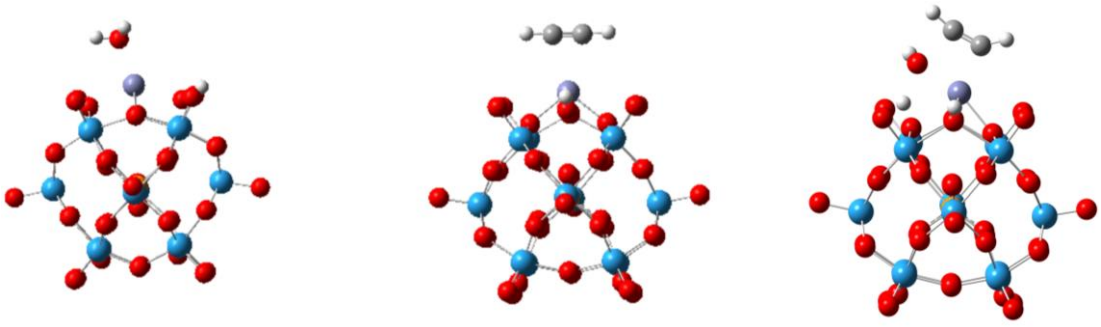

Fig. S9. Comparison of catalyst adsorption energy.

References

[1] Fukui K. Formulation of the reaction coordinate [J]. J. Phys. Chem, 1970, 74(23): 4161-3. https://doi.org/10.1021/j100717a029.

[2] Fukui K. The path of chemical reactions - the IRC approach [J]. Acc. Chem. Res, 1981, 14(12): 363-8. https://doi.org/ 10.1021/ar00072a001.

[3] Gonzalez C, Schlegel H B. Reaction path following in mass-weighted internal coordinates [J]. J. Phys. Chem, 1990, 94(14): 5523-7. https://doi.org/10.1021/j100377a021.

[4] Gonzalez C, Schlegel H B J T J O C P. An improved algorithm for reaction path following [J]. J. Phys. Chem, 1989, 90(4): 2154-61. https://doi.org/10.1063/1.456010.

[5] Jin Y Z, Gao C, Hsu W K, et al. Large-scale synthesis and characterization of carbon spheres prepared by direct pyrolysis of hydrocarbons[J]. Carbon, 2005, 43(9): 1944-1953. https://doi.org/10.1016/j.carbon.2005.03.002.

[6] Moezzi A, Cortie M, McDonagh A. Transformation of zinc hydroxide chloride monohydrate to crystalline zinc oxide[J]. Dalt. Trans, 2016, 45(17): 7385-7390. https://doi.org/10.1039/c5dt04864h.